JOURNAL OF THEORETICAL AND APPLIED MECHANICS
41, 1, pp. 19-32, Warsaw 2003

INFLUENCE OF THE COMPACT EXPLICIT FILTERING METHOD ON THE PERTURBATIONS GROWTH IN TEMPORAL SHEAR-LAYER FLOW

Artur Tyliszczak[1]

Institute of Thermal Machinery, Technical University of Częstochowa
e-mail: atyl@imc.pcz.czest.pl

In this paper the effect of the explicit filtering of high frequency phenomena performed by means of the high order compact filters is presented. A 2D unsteady incompressible flow in which the perturbations superimposed on the mean velocity profile evolve in time is considered. The dependence of the amplitudes of disturbances is analysed for various filtering procedures and compared with other methods intended to remove high frequency waves.

Key words: compact scheme, filtering, aliasing removal

1. Introduction

The widespread use and continuous development of high-speed computers turned numerical simulation a common practice for solving turbulent flow problems. This holds both for the practical industrial flows as well as for the fundamental studies where the physics of turbulence may be analysed either by direct numerical simulation (DNS) or by large eddy numerical simulation (LES). Both these methods require solution of time and length scales that differ by many orders of magnitude, starting from the large vortex structures of size of the computational domain up to the Kolmogorow scale in the case of DNS and the so-called *cut-off* scale for the LES method. From this point of view, the classical approaches based on the finite differences, finite volume or finite element methods (Hirsh, 1990) are not suitable due to their limited

[1]The author won the second prize awarded at the biennial young researchers' contest for the best work presented at the 15th Polish Conference on Fluid Mechanics, Augustów, September 2002

possibilities of solving high frequency phenomena, or eventually, their application would require a huge number of computational nodes increasing the computational time and would also require more powerful computers. Therefore, for the application of DNS and LES, the most appropriate seems to be the spectral and pseudo-spectral methods (Canuto *et al.*, 1988) for which the high resolution is obtained at a relatively small number of the computational nodes. One drawback of these methods is their limitation to the simple geometry and dependence on the type of boundary conditions. An alternate approach, which ensures spectral-like resolution is the compact scheme introduced in the 1930s. The fundamental ideas as well as their derivation techniques are, among the others, given in Vichnevetsky and Bowles (1982) and in the seminar paper of Lele (1992). The implementation of the compact scheme is relatively simple and is not restricted to the uniform grid and to some type of the boundary conditions. Moreover, it is generally more robust and less computationally costly than the spectral or pseudo-spectral methods.

The succesfull application of the compact scheme itself or its combination with the spectral and classical discretization methods has already been presented by many authors (Lele, 1992; Boersma and Lele, 1999; Cook and Riley, 1996; Metais *et al.*, 1999; Tyliszczak, 2002) for various fluid flow problems. The weak point of the compact schemes is that they do not share the so-called telescoping property, and therefore they are not conservative. It means that the system representing conservation laws at the partial differential level, when discretized by means of the compact schemes, will not reflect its conservative form at the discretization level. Moreover, except for the boundary and near boundary nodes the compact schemes have purely central character which means that they do not have dissipative properties, as for example the upwind biased scheme does. In effect, high frequency waves, arising either due to the round-of errors or the aliasing errors coming from nonlinear interaction, will grow and affect a low frequency wave what usually leads to instability, and the solution diverge. Therefore, for the computational stability it is necessary to remove or damp such errors what in practice may be done by high-pass explicit filtering which eliminate high frequency waves regardless of their source or in the case of the aliasing errors, they may be minimized by using the Arakawa (Arakawa, 1996; Peyret, 2002) skew-symmetric form of the nonlinear terms. Within this paper, based on the two-dimensional incompressible temporal shear-layer test case we compare the influence of both these methods on the growth of the disturbances in view of their amplitudes and the time of occurrence of their maximum. The flow problem chosen for the analysis assumes periodicity in one space direction allowing one in this way to use also

the pseudo-spectral approximation, which will be applied for comparison. In this case, we additionally consider the method for removing the aliasing errors by applying the 2/3 law (Canuto *et al.*, 1988).

2. Governing equations and flow configuration

The Navier-Stokes equations for the incompressible flow together with the continuity equation are given in a nondimensional form as

$$\begin{aligned} &\frac{\partial u_i}{\partial t} + \frac{\partial u_i u_j}{\partial x_j} = -\frac{1}{\rho}\frac{\partial p}{\partial x_i} + \frac{1}{\mathrm{Re}}\frac{\partial \tau_{ij}}{\partial x_j} \\ &\frac{\partial u_i}{\partial x_i} = 0 \end{aligned} \tag{2.1}$$

where

$$\tau_{ij} = \frac{\partial u_i}{\partial x_j} + \frac{\partial u_j}{\partial x_i} - \frac{2}{3}\delta_{ij}\frac{\partial u_k}{\partial x_k} \tag{2.2}$$

where Re is the Reynolds number, u_i stands for the velocity component while ρ and p denote the density and pressure, respectively. The Navier-Stokes equations $(2.1)_1$ are discretized on the uniform collocated grid with III-rd order Adams-Bashforth method for time integration. The continuity equation is enforced according to the projection method in connection with the algorithm of Ku *et al.* (1987) allowing one to fullfil the continuity equation in every computational node including the boundary nodes as well.

The flow problem considered in this work together with the prescribed boundary conditions and symbolically sketched mean velocity profile is shown in Fig. 1. The walls at the upper and lower boundary move with the speed ± 1, respectively. The mean velocity profile was taken the same as in the work of Moser and Rogers (1993) which is used for comparison and verification of the obtained results. It is given as

$$\overline{u}(y) = U\mathrm{erf}(y\sqrt{\pi}) \tag{2.3}$$

where U is the velocity outside the mixing layer. The initial disturbance superimposed on the mean velocity profile was introduced in two different ways. First, we wanted to analyse the evolution of the streamwise velocity energy spectrum in dependence of the method used to remove high frequency

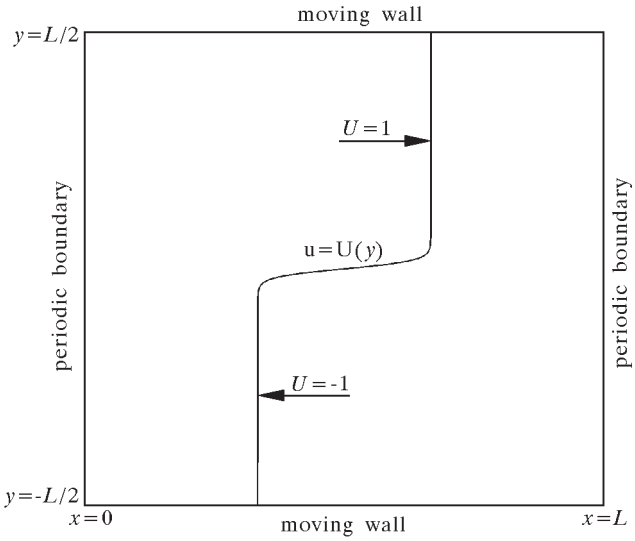

Fig. 1. Temporal shear-layer flow

phenomena. In this case, the initial velocity field was superimposed with the disturbances defined as

$$u'(y) = \sum_{k=1}^{N/4} \exp(-\pi y^2)[A_1 \cos(kx + \phi) + A_2 \sin(kx + \phi)] \tag{2.4}$$

where ϕ is the random phase shift and the amplitudes A_1, A_2 are equal to

$$A_1 = A_2 = \frac{1}{20} + \frac{1}{100}\Big(ran - \frac{1}{2}\Big) \tag{2.5}$$

where ran denotes random number in range $[0, 1]$.

The one-dimensional energy spectrum of the streamwise velocity component is defined as

$$E_1(k) = \frac{1}{L} \int_{-L/2}^{L/2} |\widehat{u}(k, y)|^2 \, dy \tag{2.6}$$

where $\widehat{u}(k, y)$ is the k-th Fourier mode.

In the next part of the computations we analysed the evolution of the particular modes explicitly defined at the initial state. In this case we disturbed the initial vorticity field $\omega(x, y) = \overline{\omega}(x, y) + \omega'(x, y)$, where $\overline{\omega}(x, y) = \partial\overline{u}(y)/\partial y$.

The vorticity disturbance is defined as

$$\omega'(x,y) = \sum_{\alpha=1,\frac{1}{2}} A_\alpha^0 \mathrm{Real}\Big[\phi_\alpha(y)\mathrm{e}^{\mathrm{i}(k_\alpha x)}\Big] \tag{2.7}$$

where the symbols $\alpha = 1, \frac{1}{2}$ are given in the form

$$\alpha = \frac{k_\alpha \lambda}{2\pi} \tag{2.8}$$

where k_α and λ denote the wave number and wavelength of the most unstable mode and its subharmonics. The length of the most unstable disturbance is equal to $\lambda = 2.32\pi$ (Moser and Rogers, 1993). The symbol A_α^0 appearing in Eq. (2.7) denotes the amplitude of a given mode, while $\phi_\alpha(y)$ represents the vorticity eigenfunction obtained from the solution of the Orr-Sommerfeld equation for the wave numbers defined according to the parameter α. The length of the computational domain L was equal four times the length of the the most unstable mode, allowing it to form four vortices corresponding to the most unstable mode, which was then subject to pairing due to the presence of the subharmonic modes (Moser and Rogers, 1993; Lesieur *et al.*, 1988). The amplitudes of a given mode of the initial perturbation or in the evolved field are measured by the integrated RMS of the velocity modes. Thus they are defined as

$$A_\alpha = \Big[\int_{-L/2}^{+L/2} 2\widehat{u}_i(\alpha)\widehat{u}_i^*(\alpha)\, dy\Big]^{\frac{1}{2}} \tag{2.9}$$

where $\widehat{u}_i(\alpha)$ is the Fourier coefficient of the velocity component u_i and $\widehat{u}_i^*(\alpha)$ is its conjugate value.

3. Space discretization method

In the computation performed, in the periodic direction we have used both the compact scheme and, also for comparison, the pseudo-spectral method (Canuto *et al.*, 1988) based on the Fourier series expansion. The approximation of the first derivative by means of the compact scheme, with the assumed uniformly spaced mesh and the nodes indexed by i, are given below. The second derivatives were computed by successive application of the first derivative approximation.

For node i the relation between the values of a function f and its derivative f' is defined [**?**] by a linear combination of both the function f and also f' as

$$\begin{aligned}&\beta f'_{i-2} + \alpha f'_{i-1} + f'_i + \alpha f'_{i+1} + \beta f'_{i+2} = \\ &= c\frac{f_{i+3} - f_{i-3}}{6h} + b\frac{f_{i+2} - f_{i-2}}{4h} + a\frac{f_{i+1} - f_{i-1}}{2h}\end{aligned} \tag{3.1}$$

where h is the mesh size. The values of the coefficients α and β together with the coefficients a, b, and c are obtained by expanding the function f and its derivative f' into Taylor series around node i, and next by matching various orders of these expansions. Note that by setting $\alpha = \beta = 0$ the explicit formula for the first derivative is obtained which formally can provide a sixth-order scheme. As shown by Lele (1992), the highest order compact approximation which can be obtained from Eq. (3.1) is of tenth order. In our computations we used the sixth-order scheme with the following values of coefficients

$$\begin{aligned}&\alpha = \frac{1}{3} \qquad && \beta = 0 \qquad && a = \frac{14}{9} \\ &b = \frac{1}{9} \qquad && c = 0\end{aligned} \tag{3.2}$$

The values of derivatives are obtained by solving the linear system of equations given as

$$\mathbf{A}\boldsymbol{f}' = \mathbf{B}\boldsymbol{f} \tag{3.3}$$

where the matrices $\mathbf{A}$ and $\mathbf{B}$ consist of the coefficients defined in Eq. (3.2). In the case of the periodic direction, the matrices $\mathbf{A}$ and $\mathbf{B}$ are of a periodic type. For the non-periodic boundaries the crucial issue of the compact schemes is the correct approximation at the boundary and near boundary nodes. While formula given by Eq. (3.1) with the set of coefficients (3.2) can be applied for the inner points starting from the node $i = 3$ up to $i = N - 2$, the approximations on $i = 1, 2$ and $i = N, N - 1$ need another treatment. We note that a wrong choice of the approximation on these nodes causes the overall approximation to violate the condition of stability based on the eigenvalues of the spatial operator – there exist eigenvalues on the right side in the complex plane of the Fourier footprint. This aspect is discussed in detail in Carpenter *et al.* (1993). According to Gustafsson (1975), who showed that the formal overall accuracy of the scheme can be at most one order higher than the order of the approximation at the boundary nodes, for our sixth order inner scheme it is advisable to use at the boundary nodes an approximation of at least fifth order. One of the possibilities to construct fifth order closure formulas at the

boundary nodes is a onesided (Lele, 1992) compact approach which can be applied to the first and second grid nodes. However, in this case the scheme violates the stability condition and can not be used. The highest possible order of the approximation obtained with compact formulas which produce a correct eigenvalue spectrum is of the form (3-4-6-4-3), where the first and last numbers stand for the order of the approximation on the boundary nodes, second and before last numbers for near boundary nodes, and the central number represents the order of the inner approximation. Thus, the overall formal approximation is of fourth order. The equations for the derivatives at the boundary nodes are given as

$$\begin{aligned} f_1' + 2f_2' &= \frac{1}{h}\Big(-\frac{15}{6}f_1 + 2f_2 + \frac{1}{2}f_3\Big) \\ f_N' + 2f_{N-1}' &= \frac{1}{h}\Big(\frac{15}{6}f_N - 2f_{N-1} - \frac{1}{2}f_{N-2}\Big) \end{aligned} \tag{3.4}$$

and for the second and before last node the equation is

$$f_{i-1}' + 4f_i' + f_{i+1}' = 3\frac{f_{i+1} - f_{i-1}}{h} \tag{3.5}$$

4. Filtering procedure

For the filtering operation we have chosen a compact filter defined (Lele, 1992) as

$$\begin{aligned} &\beta\widehat{f}_{i-2} + \alpha\widehat{f}_{i-1} + \widehat{f}_i + \alpha\widehat{f}_{i+1} + \beta\widehat{f}_{i+2} = \\ &= af_i + \frac{d}{2}(f_{i+3} + f_{i-3}) + \frac{c}{2}(f_{i+2} + f_{i-2}) + \frac{b}{2}(f_{i+1} + f_{i-1}) \end{aligned} \tag{4.1}$$

where $\widehat{f}$ stands for the filtered value at a given node. Writing the above equation for each computational node forms a system of linear equations, and their solution gives the vector of the filtered variables. The transfer function $G(\omega)$ of this filter is given as

$$G(\omega) = \frac{a + b\cos\omega + c\cos 2\omega + d\cos 3\omega}{1 + 2\alpha\cos\omega + 2\beta\cos 2\omega} \tag{4.2}$$

where $\omega = 2\pi k/N$ is the so-called scaled wave number, which for $0 \leqslant k \leqslant N/2$ belongs to the range $[0, \pi]$. The Nyquist wave number corresponds to $\omega = \pi$.

The necessary condition for the filter is to remove all the phenomena occurring at $\omega = \pi$ as they can not be solved on a given mesh. Therefore the coefficients appearing in Eq. (4.1) are determined by matching various orders of the Taylor series expansions with the additional requirement for the transfer function $G(\pi) = 0$. In the computations we have used the filters of the IV-th and VI-th order. The first one is defined by the following set of coefficients

$$a = \frac{1}{8}(5 + 6\alpha) \qquad b = \frac{1}{2}(1 + 2\alpha) \qquad c = -\frac{1}{8}(1 - 2\alpha) \tag{4.3}$$

where α varies in range $\alpha = 0.4 - 0.45$. The VI-th order filter is designed with the additional constrains for the transfer function in the form $(d^2G/d\omega^2)(\pi) = (d^4G/d\omega^4)(\pi) = 0$. These conditions cause effective damping of the wave numbers also close to $\omega = \pi$. The coefficients for this filter are defined as

$$\alpha = 0 \qquad \beta = \frac{3}{10} \qquad a = \frac{1}{2} \qquad b = \frac{3}{4} \qquad c = \frac{3}{10} \qquad d = \frac{1}{20} \tag{4.4}$$

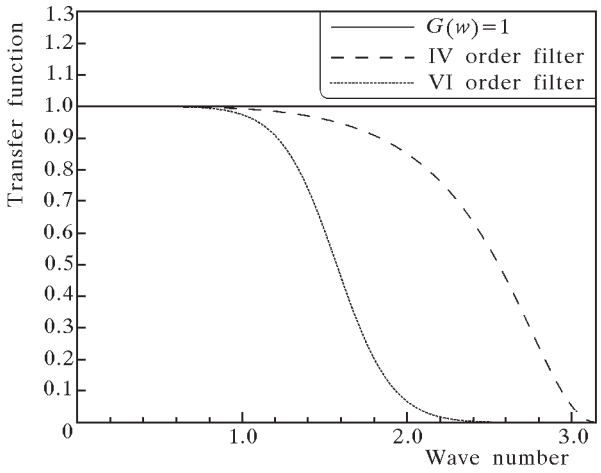

Fig. 2. Transfer function $G(\omega)$ for the IV-th order filter with $\alpha = 0.4$ and for the VI-th order filter

The transfer functions for the IV-th and VI-th order filter are shown in Fig. 2 where, as one may see, both filters have the property $G(\pi) = 0$. More-

over, the sixth-order filter will additionally damp the phenomena occurring at the high wave numbers.

In the case of non-periodic boundaries the filter given by Eq. (4.1) must be complemented by additional formulas for the boundary nodes. We have used an explicit filter of the form

$$\begin{aligned} \widehat{f}_1 &= \frac{15}{16} f_1 + \frac{1}{16}(4f_2 - 6f_3 + 4f_4 - f_5) \\ \widehat{f}_2 &= \frac{3}{4} f_2 + \frac{1}{16}(f_1 + 6f_3 - 4f_4 + f_5) \end{aligned} \tag{4.5}$$

with similar expressions for the nodes $N-1$ and N. The filter defined in Eqs (4.5) is of the IV-th order and has the property $G(\pi) = 0$.

5. Results and discussion

The computational mesh consists of 256×256 uniformly spaced nodes. The time step used in the calculation was equal to 0.01, the Reynolds number based on the vorticity thickness and the velocity outside the mixing layer was equal to 250. The amplitudes of the most unstable mode and its subharmonic mode computed according to Eq. (2.9) were equal to 0.04 and 0.03, respectively. The computations were performed for two discretization methods, first using the compact scheme in both directions (method denoted wherein as CD-CD) and also using the compact scheme in the vertical direction together with the pseudo-spectral methods in the horizontal direction (method denoted wherein as CD-PS). In the results presented below, the filtering procedure was performed every five time steps. The influence of the filtering procedure interval is not analysed in this work, but it must be stressed that it has no influence on the general trends obtained in the results presented. However, we note that without the filtering or without using another methods (e.g. Arakawa skew-symmetric form of the non-linear terms, $2/3$ law) for removing the high frequency waves, the computations are unstable. In Fig. 3 we present sample results for the computations performed with the CD-CD method showing the evolution of the vorticity.

Depending on the discretization method in a given direction, the high frequency waves have been removed in the following manner. In case of the CD-PS discretization, in the horizontal periodic direction the computations were performed with the VI-th order periodic filter, the $2/3$ law and also

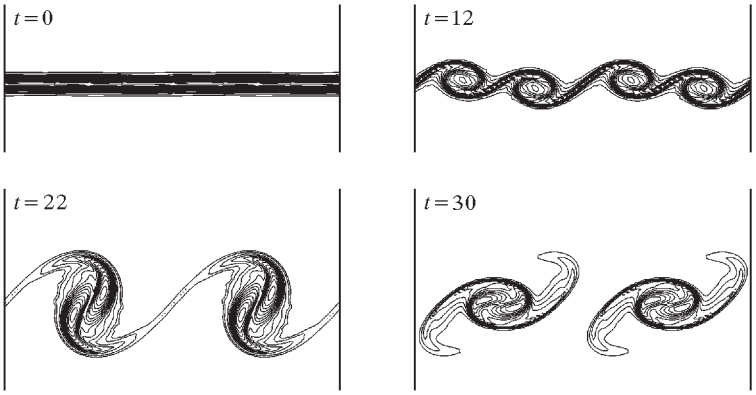

Fig. 3. The vorticity izolines for time instants $t = 0, 12, 22, 30$

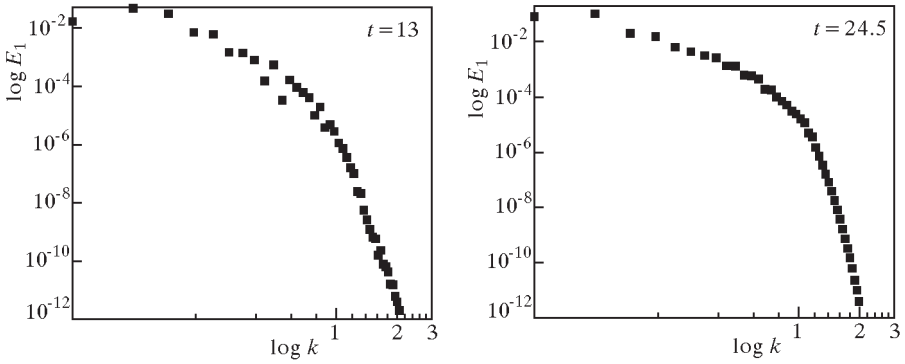

Fig. 4. Evolution of the energy spectrum for computations performed with the VI-th order periodic filter

with the Arakawa form of the nonlinear terms. In the vertical direction we applied the VI-th order filter. The computations with the CD-PS discretization method were performed for the disturbances introduced randomly as defined in Eq. (2.4). The energy spectra obtained for these computations are shown in Fig. 4 to Fig. 6. As one may see, the explicit filtering, see Fig. 4, has the best properties in the sense of removing the high frequency waves. The spectrum is smooth and there is no characteristic kink which appears at the high wave numbers in the case of the two remaining methods. The reason for this is that neither applying the 2/3 law nor Arakawa form of the nonlinear terms takes into account the viscous terms of the Navier-Stokes equations, which in fact may also produce the unresolved scale. From this point of view the explicit filtering, which does not distinguish between the source of the high frequency

phenomena, seems to be the most appropriate, however in comparison with the application of the 2/3 law, the filtering procedure is computationally a bit more costly.

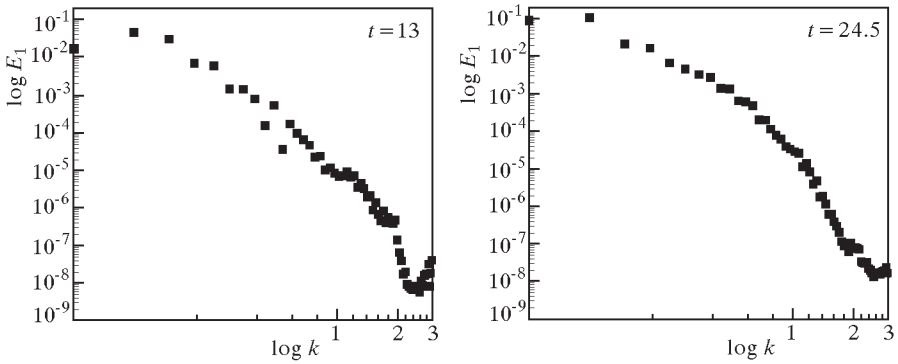

Fig. 5. Evolution of the energy spectrum for computations performed with the application of the 2/3 law

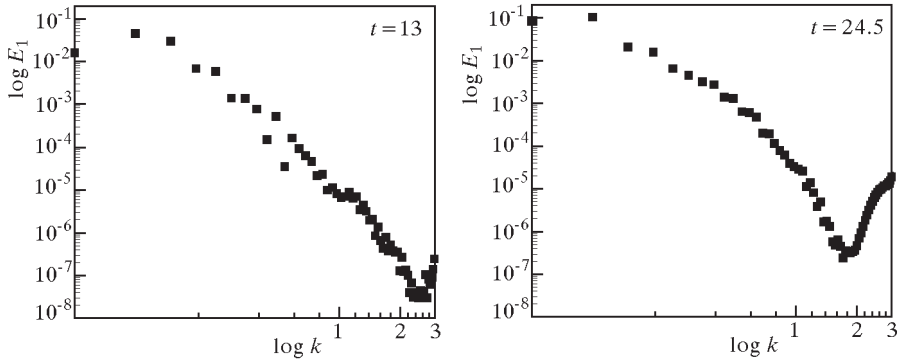

Fig. 6. Evolution of the energy spectrum for computations performed with the Arakawa form of the nonlinear terms

For the computations performed with disturbances introduced based on the eigenfunction of the Orr-Sommerfeld equation both CD-CD and CD-PS discretization methods give practically the same results, regardless of the procedure used for removing the disturbances in the periodic direction. The results presented in the following, concern the CD-CD discretization method for which in the horizontal direction we used the VI-th order filter denoted as $\mathcal{F}_x^{VI}$ while in the vertical direction we applied the Arakawa form of the nonlinear terms denoted as $\mathcal{AR}$ and the IV-th and VI-th order filters denoted as $\mathcal{F}_y^{IV}$ and $\mathcal{F}_y^{VI}$. The obtained results presenting the time evolution of the

amplitude of disturbances are shown in Fig. 7. The detailed data concerning the occurrence times of the first local maximum of the most unstable mode (denoted as t_1) and its subharmonic mode (denoted as $t_{1/2}$) together with the values of the amplitudes measured at the corresponding times are given in Table 1. These results are in good agreement with the data given in Moser and Rogers (1993) where the same flow problem has been solved with the pseudo-spectral approximation in both directions based on the Fourier/Jacobi series expansions.

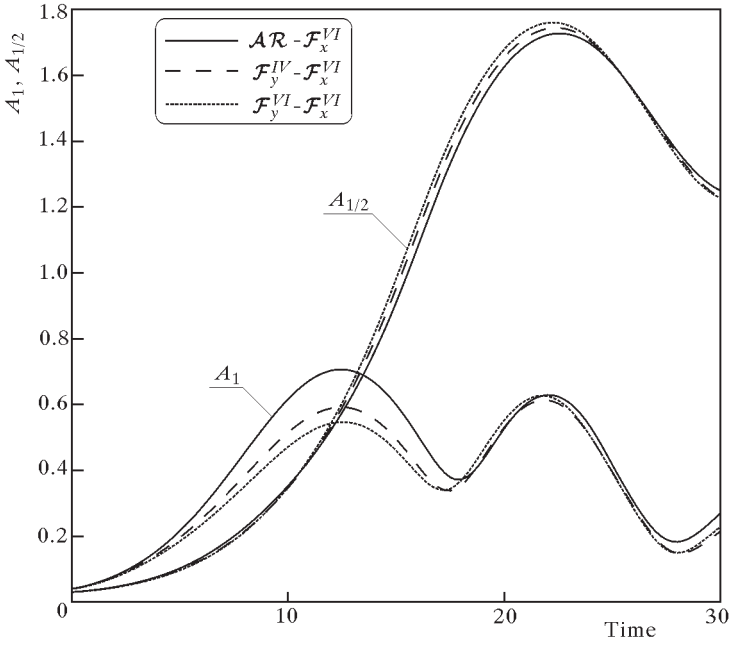

Fig. 7. Growth of the amplitude disturbances for the discretization method CD-CD for various methods used to eliminate high frequency waves

Table 1. The amplitudes A_1 and $A_{1/2}$ and the occurrence time of their maxima for the CD-CD discretization method

	A_1	t_1	$A_{1/2}$	$t_{1/2}$
$\mathcal{AR} - \mathcal{F}_x^{VI}$	0.707	12.50	1.727	22.50
$\mathcal{F}_y^{IV} - \mathcal{F}_x^{VI}$	0.591	12.25	1.744	22.50
$\mathcal{F}_y^{VI} - \mathcal{F}_x^{VI}$	0.547	12.50	1.760	22.25

In this paper there was no data concerning the values of the amplitudes, while the presented times t_1 and $t_{1/2}$ were equal to 11.9 and 21.5, respectively. The results shown in Fig. 7 confirm good properties of the filtering procedure. In comparison to the results obtained with the Arakawa form of the nonlinear terms, the amplitude of the high frequency disturbance A_1, which in this case is the most unstable mode, is decreased. Furthermore, applying the VI-th order filter, which has the property to completely remove not only the waves corresponding to Nyquist frequency but also the waves close to it, see Fig. 2, allows for the most efficient damping of the high frequency phenomena. The important thing is that none of the filters considerably influence neither the time of the local amplitude maxima nor the low frequency waves. The amplitude of the subharmonic disturbance is almost the same for all the method applied.

This work was supported by State Committee for Scientific Research, Poland, under grant No. 8 T10B 009 19.

References

1. ARAKAWA A., 1966, Computational design for long-term numerical integration of the equations of fluid motion: Two dimensional incompressible flow. Part 1, *Journal of Computational Physics*, **1**, 119-143

2. BOERSMA B.J., LELE S.K., 1999, Large eddy simulation of compressible jet, *Annual Research Briefs*, Stanford University Center for Turbulence Research

3. CANUTO C., HUSSAINI M.Y., QUARTERONI A., ZANG T.A., 1988, *Spectral Methods in Fluid Dynamics*, Springer-Verlag

4. CARPENTER M.H., GOTTLIEB D., ABARBANEL S., 1993, The stability of numerical boundary treatements for compact high-order finite-difference schemes, *Journal of Computational Physics*, **108**, 272-295

5. COOK W.C., RILEY J.J., 1996, Direct numerical simulation of a turbulent reactive plume on a parallel computer, *Journal of Computational Physics*, **129**, 263-283

6. GUSTAFSSON B., 1975, The convergence rate for difference approximations to mixed initial boundary value problems, *Math. Comput.*, **29**, 396-406

7. HIRSH CH., 1990, *Numerical Computation of Internal and External Flows*, John Wiley & Sons, Chichester

8. Ku H.C., Hirsh R.S., Taylor T.D., 1987, Pseudospectral methods for solution of the incompressible Navier-Stokes equations, *Computers and Fluids*, **15**, 195-214

9. Lele S.K., 1992, Compact finite difference with spectral-like resolution, *Journal of Computational Physics*, **103**, 16-42

10. Lesieur M., Staquet Ch., Le Roy P., Comte P., 1988, The mixing layer and its coherence examined from the point of view of two-dimensional turbulence, *Journal of Fluid Mechanics*, **192**, 511-534

11. Metais O., Lesieur M., Comte P., 1999, *Transition, Turbulence and Combastion Modelling, Chapter – Large-Eddy Simulations of Incompressible and Compressible Turbulence*, KLUWER Academic Publisher

12. Moser R.D., Rogers M.M., 1993, The three-dimensional evolution of a plane mixing layer: pairing and transition to turbulence, *Journal of Fluid Mechanics*, **247**, 275-320

13. Peyret R., 2002, *Spectral Methods for Incompressible Viscous Flow*, Springer-Verlag New York

14. Tyliszczak A., 2002, Application of preconditioning methods for compressible flows, PhD thesis, Politechnika Częstochowska/von Kármán Institute for Fluid Dynamics

15. Vichnevetsky R., Bowles J.B., 1982, Fourier analysis of numerical approximations of hyperbolic equations, *SIAM*, Philadelphia

Wpływ jawnej filtracji metodą kompaktową na wzrost zaburzeń w nieustalonym przepływie z warstwą ścinającą

Streszczenie

W pracy przedstawiono efektywność jawnej filtracji zjawisk wysokoczęstotliwościowych przy zastosowaniu filtracji kompaktowej. Analizie poddano nieściśliwy dwuwymiarowy przepływ z warstwą ścinającą w którym rozpatrywano ewolucję zaburzeń nałożonych na pole prędkości średniej. Przedstawiono porównania wartości amplitud zaburzeń obliczonych przy zastosowaniu różnych procedur filtracji oraz dla innych metod stosowanych do eliminowania zjawisk wysokoczestotliwościowych.

Manuscript received November 18, 2002; accepted for print November 27, 2002